Cut-Off Effects on the QCD Thermal Transition as a Function of Quark Masses and Chemical Potential

F. Cuteri, O. Philipsen, A. Schön, A. Sciarra

published in

NIC Symposium 2020
M. Müller, K. Binder, A. Trautmann (Editors)

Forschungszentrum Jülich GmbH,
John von Neumann Institute for Computing (NIC),
Schriften des Forschungszentrums Jülich, NIC Series, Vol. 50,
ISBN 978-3-95806-443-0, pp. 33.
http://hdl.handle.net/2128/24435

Cut-Off Effects on the QCD Thermal Transition as a Function of Quark Masses and Chemical Potential

Francesca Cuteri[1], **Owe Philipsen**[1,2], **Alena Schön**[1], **and Alessandro Sciarra**[1]

[1] Institut für Theoretische Physik, Goethe Universität Frankfurt,
Max-von-Laue-Str. 1, 60438 Frankfurt, Germany
E-mail: {*cuteri, philipsen, schoen, sciarra*}*@th.physik.uni-frankfurt.de*

[2] John von Neumann Institute for Computing (NIC), GSI, Planckstr. 1, 64291 Darmstadt, Germany

We report on the status of a long term project to determine the nature of the thermal transition in QCD (the fundamental theory of strongly interacting matter composed of quarks and gluons) as a function of the number of quark flavours, their masses, imaginary chemical potential for baryon number and the lattice spacing. Our knowledge on the order of the thermal QCD transition depending on these parameters is summarised in what is known as *Columbia plot*. Besides showing the structure of the theory, it is important to constrain the QCD phase diagram realised by nature, which cannot be simulated directly due to a severe sign problem at real baryon chemical potentials. Having determined the qualitative structure of the Colombia plot in earlier studies, current efforts focus on reducing the lattice spacing and understanding discretisation effects, which need to be removed to arrive at continuum results.

1 Introduction

Quantum Chromodynamics is the fundamental theory of the strong interactions governing the forces between nuclear and subnuclear particles. Its fundamental degrees of freedom are light u- and d-quarks, a heavier s-quark and gluons, which are the force carriers in this quantum field theory. The coupling strength of the interactions depends on the energy scale of a scattering process. For energies below a few GeV, the coupling is large and quarks and gluons combine into numerous tightly bound states, the hadrons, among them the familiar proton and neutron. On the other hand, at large temperatures or densities, the average energy per particle is higher and the theory enters a weak coupling regime, where the constituents form a so-called quark gluon plasma. The QCD phase diagram determines the form of matter under different conditions as a function of temperature, T, and matter density parametrised by a chemical potential μ for quark number, which is one third that of the conserved baryon number. Whether and where the hadronic phase and the quark gluon plasma are separated by true phase transitions has to be determined by first principle calculations and experiments. Since QCD is strongly coupled on scales of hadronic matter, a non-perturbative treatment is necessary. The most reliable approach is by Monte Carlo simulation of a reformulation of the theory on a space-time grid, lattice QCD.

Unfortunately, the so-called sign problem prohibits straightforward simulations at finite baryon density. For this reason, knowledge of the thermal phase transition at zero density as a function of the theory's parameters, also for unphysical values, is of great importance to constrain and anchor research in the finite density direction. It is well-known that the physical point of QCD (with quark mass values realised in nature) displays only an analytic, smooth crossover between the hadronic and the plasma regions, without a non-analytic phase transition.[1] However, the order of the finite temperature phase transition at

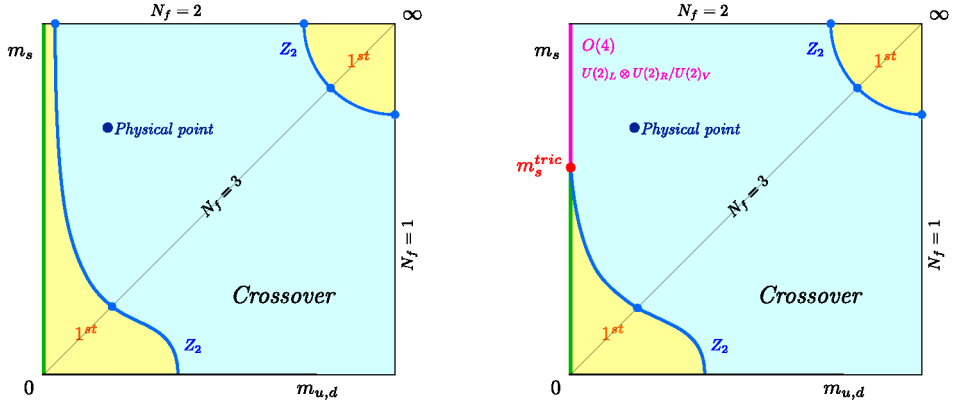

(a) First order scenario in the $m_s - m_{u,d}$ plane

(b) Second order scenario in the $m_s - m_{u,d}$ plane

Figure 1. Two possible scenarios for the order of the QCD thermal phase transition as a function of the quarks masses. Indicated in Fig. 1(b) are also plausible universality classes for the second order line at $m_{u,d} = 0$.

zero density depends on the quark masses as is schematically shown in Fig. 1(a), where N_f denotes the number of mass degenerate quark flavours. In the limits of zero and infinite quark masses (lower left and upper right corners), order parameters corresponding to the breaking of some global symmetry can be defined, and for three degenerate quarks one numerically finds, on rather coarse lattices, first order phase transitions at small and large quark masses at some finite temperatures $T_c(m)$. On the other hand, one observes an analytic crossover at intermediate quark masses, with second order boundary lines separating these regions. Both lines have been shown to belong to the $Z(2)$ universality class of the 3d Ising model.[2–4] The critical lines delimit the quark mass regions featuring a chiral or deconfinement phase transition, and are called chiral and deconfinement critical lines, respectively. The former has been mapped out on $N_\tau = 4$ lattices[5] and puts the physical quark mass configuration in the crossover region. The chiral critical line recedes with decreasing lattice spacing,[6, 7] which is parametrised by increasing temporal lattice extent N_τ (see below): for $N_f = 3$, on the critical point, the quark masses correspond to pion mass values $m_\pi(N_\tau = 4)/m_\pi(N_\tau = 6) \sim 1.8$. Thus, in the continuum the physical point is deeper in the crossover region than on coarse lattices. An open question to this day remains the order of the transition in the limit of zero light quark masses, called the chiral limit. As explained below, this limit cannot be directly simulated. Consequently, it is still not known whether the chiral phase transition for two quark flavours is of first or second order. Hence an alternative scenario is Fig. 1(b). Clarifying this question is important because of the proximity of the critical line to the physical point.

2 The General Strategy

All numerical simulations have been performed using the publicly available[8] OpenCL-based code CL^{2}QCD,[9] which is optimised to run efficiently on AMD GPUs and provides,

	Crossover	1^{st} triple	Tricritical	$3D$ Ising
B_4	3	1.5	2	1.604
ν	–	1/3	1/2	0.6301(4)

Table 1. Critical values of ν and $B_4 \equiv B_4(\beta_c, X_c, \infty)$ for some universality classes.[11]

among other features, an implementation of the (R)HMC algorithm for unimproved (rooted staggered) Wilson fermions.

In our studies, the chemical potential has been kept fixed at either $\mu = 0$ or at the purely imaginary value $\mu = i\mu_i^{RW}, \mu_i^{RW} = \pi/3$. The latter choice is motivated by the fact that there is no sign problem at imaginary chemical potential, and that μ_i^{RW} constitutes a Roberge-Weiss phase boundary between different centre-sectors of the QCD symmetry group, which are periodically repeated as imaginary chemical potential is increased.[10]

Temperature T is related to the lattice gauge coupling β and the temporal lattice extent according to

$$T = 1/(a(\beta)N_\tau) \tag{1}$$

Approaching the continuum limit at fixed temperature is realised by taking $\beta \to \infty$, $a(\beta) \to 0, N_\tau \to \infty$. Our studies in Sec. 5 and in Sec. 4 are conducted at a fixed temporal extent N_τ of the lattices (no continuum limit is attempted in these cases), while for the study described in Sec. 3 three different values of N_τ are considered. The ranges in mass m or hopping parameter κ (parametrising mass in the Wilson discretisation) and gauge coupling constant β are always dictated by our purpose of locating the chiral/deconfinement phase transition.

In order to locate the chiral/deconfinement phase transition and to identify its order, a common strategy is adopted, which consists of a finite size scaling analysis (FSS) of the third and/or fourth standardised moments of the distribution of an order parameter for the transition. The n$^{\text{th}}$ standardised moment, given the distribution of a generic observable $\mathcal{O}$, is expressed as

$$B_n(\mathcal{O}) = \frac{\langle (\mathcal{O} - \langle \mathcal{O} \rangle)^n \rangle}{\left\langle (\mathcal{O} - \langle \mathcal{O} \rangle)^2 \right\rangle^{n/2}} \tag{2}$$

and we analyse its dependence on some parameter $X \in \{m, \kappa, \beta\}$ and on the volume. We will introduce an exact or approximate order parameter $\mathcal{O}$ for each investigation in the corresponding sections. However, in all cases, in order to extract the order of the transition as a function of the bare quark mass and/or number of flavours, we considered the kurtosis $B_4(\mathcal{O})$ of the sampled distribution of $\mathcal{O}$.

In the thermodynamic limit $N_\sigma \to \infty$, the universal values taken by the kurtosis B_4 and by the critical exponent ν for our cases of interest are well known results listed in Tab. 1. However, the discontinuous step function characterising the thermodynamic limit is smeared out to a smooth function as soon as a finite volume is considered and a FSS is needed. In all cases we varied the spatial extent of the lattice N_σ such that the aspect ratios, governing the size of the box in physical units at finite temperature, was in the range

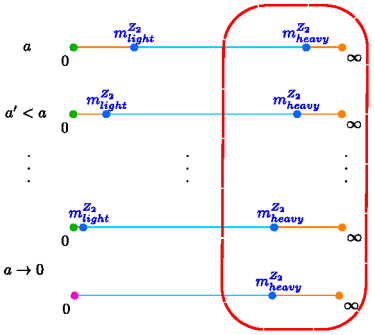

(a) Shift of the critical m_{Z_2} masses at $N_{\rm f} = 2$ towards the continuum limit

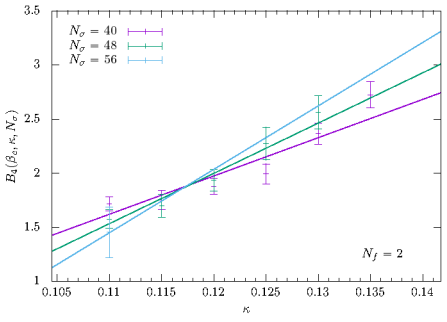

(b) FSS of B_4 and fit

Figure 2. Features and preliminary results on the Z_2 boundary in the high mass corner of the Columbia plot.

$N_\sigma/N_\tau \in [2-5]$. In the vicinity of a critical point, the kurtosis can be expanded in powers of the scaling variable $x = (X - X_c)N_\sigma^{1/\nu}$ and, for large enough volumes, the expansion can be truncated after the linear term,

$$B_4(\beta_c, X, N_\sigma) \simeq B_4(\beta_c, X_c, \infty) + c(X - X_c)N_\sigma^{1/\nu} \tag{3}$$

In our case, for the studies described in Sec. 3 and in Sec. 4, the critical value for $X_c = \kappa, m$ corresponds to a second order phase transition in the 3D Ising universality class, so that one can fix $B_4 \approx 1.604$ and $\nu \approx 0.63$ and perform the fit to Eq. 3 with the sole aim of extracting X_c (and c).

3 Updates on the Columbia Plot: Z_2 Boundary in the High Mass Corner

The cut-off effects that quantitatively affect our picture of the QCD phase structure have been investigated in previous studies in the upper right corner of the Columbia plot, and the Z_2 transitions were already observed to shift to smaller masses for $N_{\rm f} = 2, 2+1, 3$ at $\mu = 0$.[6, 12–14] A sketch of this behaviour for $N_{\rm f} = 2$ is given in Fig. 2(a). No continuum extrapolation is available yet.

In this case the norm of the Polyakov loop, $||L||$, was used as approximate order parameter for the deconfinement phase transition. The case of $N_{\rm f} = 2$ degenerate quarks was addressed and, with a scan in κ, the location of the critical $\kappa_{\rm heavy}^{Z_2}$ endpoint on $N_\tau = 6, 8, 10$

N_τ	$\kappa_{\rm heavy}^{Z_2}$	a [fm]	am_π	m_π [MeV]	V_{min} [fm^3]	L_{min} [fm]
6	0.0834(64)	[0.1175(6):0.1232(5)]	[3.4709(3):2.2411(3)]	[5910(30):3638(15)]	76	4.23
8	0.1145(32)	[0.0882(4):0.0960(8)]	[2.1310(6):1.2325(4)]	[4830(20):2570(20)]	44	3.54
10	0.1255(43)	[0.0690(10):0.0762(11)]	[1.8734(3):0.9284(5)]	[5430(80):2440(40)]	42	3.49

Table 2. Results on $V_{\rm min}$ from fits of the kurtosis.

was investigated with the aim to monitor and possibly model cut-off effects. A previous report on this project is to be found in Ref. 15, while here we focus on the impact of finite size effects in this investigation. It is an additional difficulty of the heavy mass region that pions cannot be resolved on our lattices up to $N_\tau \approx 10$. And, while $a \to 0$ with growing N_τ, the necessity of keeping the relation $1 \ll N_\tau \ll N_\sigma$ satisfied forces us to use larger N_σ values to keep the size of the box fixed in physical units. This has to be satisfied already for the smallest of the volumes in our FSS analysis.

In view of the increasing cost of simulations, some work was invested in devising an alternative and possibly cheaper strategy to locate $\kappa_{\text{heavy}}^{Z_2}$. One could, indeed, first identify at any fixed value of the bare mass some *minimal physical volume* V_{min}, characterised by that it allows a reliable extraction of $\kappa_{\text{heavy}}^{Z_2}$ from a linear fit of the kurtosis. At a different κ or N_τ, it should then be enough to *e. g.* reweight the effective potential V_{eff} at just one fixed $V \gtrsim V_{\text{min}}$ as in Ref. 13 to locate the phase transition and understand its nature. In practice we start by using a modified fit ansatz for the kurtosis in the vicinity of the critical point[16]

$$B_4(\kappa, N_\sigma) = \left[B_4(\kappa_{\text{heavy}}^{Z_2}, \infty) + c\,(\kappa - \kappa_{\text{heavy}}^{Z_2}) N_\sigma^{(1/\nu)} \right] (1 + B N_\sigma^{y_t - y_h})$$

which incorporates the finite volume effect for generic observables which are a mixture of energy-like and magnetisation-like operator and where the value of the exponent $y_t - y_h$ is fixed by universality. Then we estimate V_{min} by excluding one-by-one the smallest physical volumes in the fit, until the value of the coefficient of the correction term is compatible with zero. Preliminary results are collected in Tab. 2 and one example of the performed fits is provided in Fig. 2(b).

4 Updates on an Alternative $m_{u,d}$–N_{f} Columbia Plot: Z_2 Boundary in the Chiral Limit

In this study we treat N_{f} as a continuous real parameter of some statistical system behaving, at any integer N_{f} value, as QCD at zero density, with N_{f} mass-degenerate fermion species[17]

$$Z_{N_{\text{f}}}(m) = \int \mathcal{D}U \left[\det M(U, m)\right]^{N_{\text{f}}} e^{-\mathcal{S}_{\text{G}}} \tag{4}$$

Within this framework, the two considered scenarios for the Columbia plot can be put in one-to-one correspondence with the two sketches for the order of the thermal phase transition in the (m, N_{f})-plane displayed in Fig. 3.

We employ unimproved staggered fermions and use the RHMC algorithm[18] to simulate any number N_{f} of degenerate flavours. Our original strategy was to find out for which tricritical value $N_{\text{f}}^{\text{tric}}$ the phase transition displayed by this system changes from first-order to second-order, by mapping out the Z_2 phase boundary. The extrapolation to the chiral limit with known tricritical exponents can then decide between the two scenarios, depending on whether $N_{\text{f}}^{\text{tric}}$ is larger or smaller than 2.

While the tricritical scaling region was found to be very narrow already on coarse $N_\tau = 4$ lattices, results at larger m and N_{f} were found to feature, over a much wider region, a remarkable linear behaviour, which was not expected on universality grounds, see Fig. 4 .

What our findings suggest is that, if it is reasonable to expect both linearity within some range in N_{f} and tricritical scaling more in the chiral limit, then one would be able to make

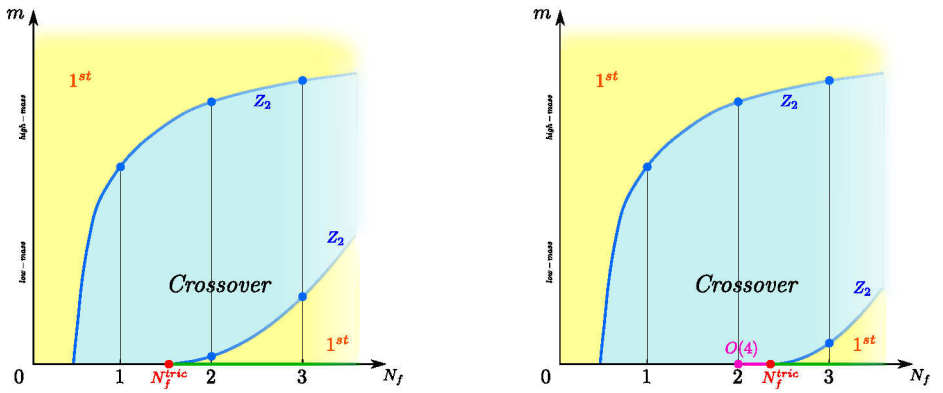

(a) First order scenario in the $m_{u,d} - N_{\rm f}$ plane

(b) Second order scenario in the $m_{u,d} - N_{\rm f}$ plane

Figure 3. The two considered possible scenarios for the order of the QCD thermal phase transition as a function of the light-quarks mass and the number of fermion flavours.

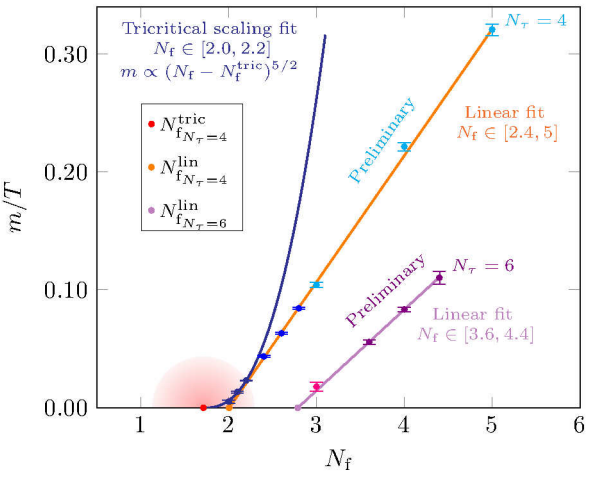

Figure 4. The Z_2 boundary in the $m/T - N_{\rm f}$ plane for $N_\tau = 4, 6$. The dark blue line represents the tricritical extrapolation to the chiral limit as in Ref. 17. The orange line represents a linear extrapolation based on m_{Z_2} in the $N_{\rm f}$ range $2.4 - 5$ using also newly simulated points. The violet line represents a linear extrapolation on the basis of m_{Z_2} in the $N_{\rm f}$ range $3.6 - 4.4$. The magenta point at $N_\tau = 6$ and $N_{\rm f} = 3$ is borrowed from Ref. 6.

use of a linear extrapolation to $m = 0$, to at least get $N_{\rm f}^{\rm lin}$ as an upper bound for $N_{\rm f}^{\rm tric}$, out of much more affordable simulations and possibly without even simulating at noninteger numbers of flavours.

For as long as the upper bound from the linear extrapolation keeps lying at $N_{\rm f} < 2$, while one simulates at larger and larger N_τ values towards the continuum limit, one can

infer that the transition in the $N_{\rm f} = 2$ chiral limit is of first order. However, should our linear extrapolation give $N_{\rm f}^{\rm lin} \gtrsim 2$, then knowledge of the size of the scaling region is necessary to draw conclusions.

Our results are reported in Fig. 4. The first important thing to observe is that, while tricritical extrapolation for $N_\tau = 4$ resulted in $N_{\rm f}^{\rm tric} < 2$, providing an independent confirmation for the first order scenario being realised on coarse lattices, a linear extrapolation to the chiral limit using $N_{\rm f} \in [2.4, 5.0]$, results in $N_{\rm f}^{\rm lin} = 2$ within errors. Strictly speaking, by just considering $N_\tau = 4$ results, one would conclude that the linear extrapolation alone cannot give conclusive answers on the order of the $N_{\rm f} = 2$ transition in the chiral limit. However, results on finer lattices were produced as well. On $N_\tau = 6$, what we observe is that data within the range $N_{\rm f} \in [3.6, 4.4]$ certainly do not fall in the tricritical scaling region, but they do exhibit linear scaling. Moreover, if we consider the result for $N_{\rm f} = 3$ for the same discretisation from the literature,[6] we can see it is fully consistent with our linear extrapolation. Finally, the most important aspect of this result is that, linearly extrapolating at $N_\tau = 6$, we get $N_{\rm f}^{\rm lin} \lesssim 3$, namely quite far to the right of $N_{\rm f} = 2$.

5 Updates on the Extended Columbia Plot: Roberge-Weiss Endpoint

The Columbia plot at $\mu_i = \mu_i^{RW}$ displayed in Fig. 5(a) looks similar to the one in Fig. 1(a), but with the Z_2 lines replaced by tricritical lines, first order triple regions that are wider than at $\mu = 0$ and a second order Z_2 region at intermediate values for the quark masses. In this case the imaginary part of the Polyakov loop $L_{\rm Im}$ was measured as order parameter for the Roberge-Weiss phase transition. Once again, we focused on the case of $N_{\rm f} = 2$ degenerate unimproved staggered quarks, and tried to locate, with a scan in mass, the tricritical points $m_{\rm heavy}^{\rm tricr.}$ and $m_{\rm light}^{\rm tricr.}$ on $N_\tau = 6$ lattices as already done for other discretisations and N_τ values.[19–21] A previous report on this project is to be found in Ref. 23.

For each value of $m_{u,d}$, simulations were performed at a fixed temporal lattice extent $N_\tau = 6$ and at a fixed value of the chemical potential $a\mu_i^{RW} = \pi/6$. The extraction of the critical exponent ν was accomplished both with the kurtosis fit procedure and with a quantitative data collapse described in Ref. 24. Results for the critical exponent ν are reported in Fig. 5(b). Since results from either kind of analysis happen to agree within a 1σ discrepancy in all (but one) case, they are combined to obtain the final answer on ν. To comment more on our results, it is important to stress that for the FSS at least three volumes are necessary for safe conclusions and we used $N_\sigma^{\rm min} = 12, 18, 24$ and $N_\sigma^{\rm max} = 30, 36, 42$, depending on the mass. For each lattice size, 3 to 8 values of β around the critical temperature were simulated, each with 4 Markov chains.

In order to decide when to stop accumulating statistics, for large (small) masses the kurtosis of the imaginary part of Polyakov loop was required to be compatible on all the chains within 2 (3) standard deviations. Since this condition can be fulfilled also at a very poor statistics, due to large errors, a further empirical requirement is that values of the kurtosis from different chains must span, errors included, an interval not wider than 0.5.

As indicated in Fig. 5(b) it is still not possible to give the two tricritical masses with their statistical error, because in the light mass range no simulation point falls on the first order triple line. This is because larger and larger volumes are needed in ranges where the transition goes from tricritical to weakly first-order. We can however quote a result with asymmetric errors to reflect this uncertainty, $m_{\pi{\rm light}}^{\rm tricr.} = 328^{+44}_{-88}$ MeV.[24] One can now

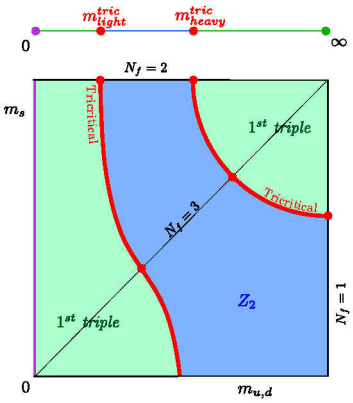

(a) The Columbia plot of the Roberge-Weiss plane, *i. e.* the order of the thermal phase transition in the $m_s - m_{u,d}$ plane at $\mu_i = \mu_i^{RW}$. The $N_f = 2$ case is highlighted.

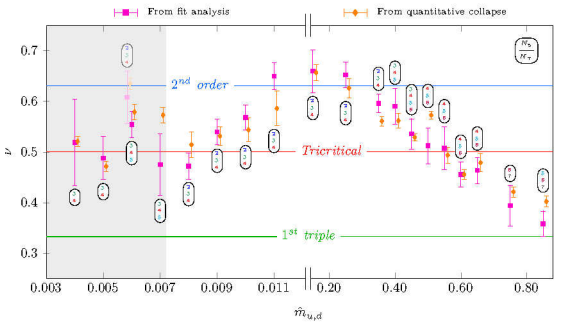

(b) Critical exponent ν as a function of the bare quark mass m. For the sake of readability, the mass axis has been broken and two different scales have been used. Shaded points correspond to preliminary results for which higher statistics is needed.

Figure 5. Features and preliminary results on the tricritical endpoints in the Roberge-Weiss Columbia plot.

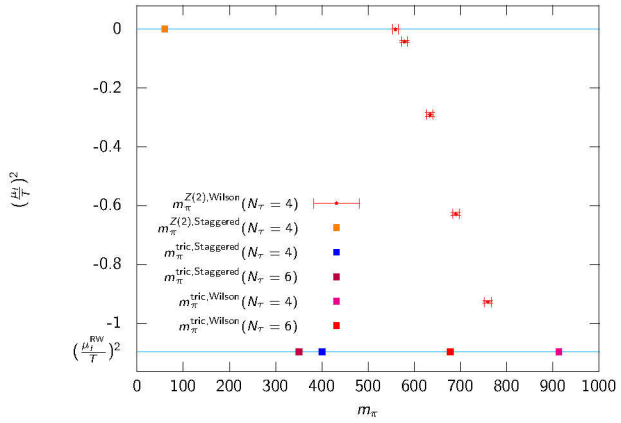

Figure 6. Collection of results on the Z_2 critical line/points in the $m_\pi - \mu^2$ plane. Results from various discretisations and different N_τ can be compared.[19, 20, 22, 25, 26]

compare with results from other discretisations and/or at other N_τ values, as we do in Fig. 6. We now clearly see the shift of $m_{\pi\text{light}}^{\text{tricr.}}$ towards smaller masses when going from $N_\tau = 4$ to $N_\tau = 6$. One can also compare the Wilson *versus* staggered discretisations: the shift amounts to 35 % (14 %) of the value for Wilson (staggered). At large masses the value found for $m_{\pi\text{ heavy}}^{\text{tricr.}}$ is still affected by large cut-off effects, as indicated by $am_\pi > 1$. This means finer lattices are necessary to resolve the pion.

6 Conclusions

Our systematic study of the order of the QCD thermal transition and its dependence on the parameters of the theory as well as on the simulation volume and lattice spacing has revealed two main insights: the first of these is rather unfortunate technically, as it indicates very strong cut-off effects on the second-order boundary lines in the Columbia plot, both at zero and non-zero baryon density. Combined with the large volumes required to decide on the order of the transition, this renders future investigations extremely compute-expensive, and thus slow, before one can extrapolate to the desired continuum results. On the positive side, we have at least arrived at a full understanding of the qualitative features of cut-off effects on the Columbia plot. In particular, the chiral first-order region shrinks strongly with decreasing lattice spacing, for all N_f and at zero as well as non-zero baryon density. This is valuable input also to constrain the physical QCD phase diagram. Finally, at least in the heavy mass region one might hope to find a continuum limit for the second-order boundary within the next couple of years, which would serve as valuable benchmark for, *e. g.* functional renormalisation group methods in the continuum.

Acknowledgements

This work was partially funded by the Deutsche Forschungsgemeinschaft (DFG, German Research Foundation), project number 315477589 -TRR 211. We also acknowledge support by the Helmholtz International Center for FAIR within the LOEWE program of the State of Hesse.

References

1. Y. Aoki, G. Endrődi, Z. Fodor, S. D. Katz, and K. K. Szabo, *The Order of the quantum chromodynamics transition predicted by the standard model of particle physics*, Nature **443**, 675, 2006.
2. F. Karsch, E. Laermann, and C. Schmidt, *The Chiral critical point in three-flavor QCD*, Phys. Lett. B **520**, 41, 2001.
3. P. de Forcrand and O. Philipsen, *The QCD phase diagram for three degenerate flavors and small baryon density*, Nucl. Phys. B **673**, 170, 2003.
4. S. Kim, P. de Forcrand, S. Kratochvila, and T. Takaishi, *The 3-state Potts model as a heavy quark finite density laboratory*, PoS LAT **2005**, 166, 2006.
5. P. de Forcrand and O. Philipsen, *The Chiral critical line of N(f) = 2+1 QCD at zero and non-zero baryon density*, JHEP **0701**, 077, 2007.
6. P. de Forcrand, S. Kim, and O. Philipsen, *A QCD chiral critical point at small chemical potential: Is it there or not?*, PoS LAT **2007**, 178, 2007.
7. G. Endrodi, Z. Fodor, S. D. Katz, and K. K. Szabo, *The Nature of the finite temperature QCD transition as a function of the quark masses*, PoS LAT **2007**, 182, 2007.
8. M. Bach, F. Cuteri, C. Czaban, C. Pinke, A. Sciarra *et al.*, *CL^{2}QCD: lattice QCD using OpenCL* (since 2011), `https://github.com/AG-Philipsen/cl2qcd`.
9. O. Philipsen, C. Pinke, A. Sciarra, and M. Bach, *CL^{2}QCD - Lattice QCD based on OpenCL*, PoS LAT **2014**, 038, 2014.

10. A. Roberge and N. Weiss, *Gauge Theories With Imaginary Chemical Potential and the Phases of QCD*, Nucl. Phys. B **275**,734 , 1986, doi:10.1016/0550-3213(86)90582-1.
11. A. Pelissetto and E. Vicari, *Critical phenomena and renormalization group theory*, Phys. Rept. **368**, 549, 2002.
12. P. de Forcrand and O. Philipsen, *The curvature of the critical surface $(m_{ud}, m_s)^{crit}(\mu)$: a progress report*, PoS LAT **2008**, 208, 2008, arXiv:0811.3858 [hep-lat].
13. H. Saito, S. Ejiri, S. Aoki, T. Hatsuda, K. Kanaya, Y. Maezawa, H. Ohno, and T. Umeda (WHOT-QCD Collaboration), *Phase structure of finite temperature QCD in the heavy quark region*, Phys. Rev. D **84**, 054502, 2011, [Erratum: Phys. Rev. D **85**, 079902, 2012], arXiv:1106.0974 [hep-lat].
14. M. Fromm, J. Langelage, S. Lottini, and O. Philipsen, *The QCD deconfinement transition for heavy quarks and all baryon chemical potentials*, JHEP **01**, 042, 2012, arXiv:1111.4953 [hep-lat].
15. C. Czaban and O. Philipsen, *The QCD deconfinement critical point for $N_\tau = 8$ with $N_f = 2$ flavours of unimproved Wilson fermions*, PoS LAT **2016**, 056, 2016, arXiv:1609.05745 [hep-lat].
16. X. Y. Jin, Y. Kuramashi, Y. Nakamura, S. Takeda, and A. Ukawa, *Critical point phase transition for finite temperature 3-flavor QCD with nonperturbatively O(a) improved Wilson fermions at $N_t = 10$*, Phys. Rev. D **96**, 034523, 2017, arXiv:1706.01178 [hep-lat].
17. F. Cuteri, O. Philipsen, and A. Sciarra, *The QCD chiral phase transition from non-integer numbers of flavors*, Phys. Rev. D **97**, 114511, 2018, arXiv:1711.05658 [hep-lat].
18. A. D. Kennedy, I. Horvath, and S. Sint, Nucl. Phys. Proc. Suppl. **73**, 834, 1999, arXiv:hep-lat/9809092.
19. O. Philipsen and C. Pinke, *The nature of the Roberge-Weiss transition in $N_f = 2$ QCD with Wilson fermions*, Phys. Rev. D **89**, 094504, 2014, arXiv:1402.0838 [hep-lat].
20. C. Czaban, F. Cuteri, O. Philipsen, C. Pinke, and A. Sciarra, *Roberge-Weiss transition in $N_f = 2$ QCD with Wilson fermions and $N_\tau = 6$*, Phys. Rev. D **93**, 054507, 2016, arXiv:1512.07180 [hep-lat].
21. C. Bonati, G. Cossu, M. D'Elia, and F. Sanfilippo, *Roberge-Weiss endpoint in $N_f = 2$ QCD*, Phys. Rev. D **83**, 054505, 2011.
22. C. Bonati, P. de Forcrand, M. D'Elia, O. Philipsen, and F. Sanfilippo, *Chiral phase transition in two-flavor QCD from an imaginary chemical potential*, Phys. Rev. D **90**, 074030, 2014.
23. O. Philipsen and A. Sciarra, *Roberge-Weiss transition in $N_f = 2$ QCD with staggered fermions and $N_\tau = 6$*, PoS LAT **2016**, 055, 2016, arXiv:1610.09979 [hep-lat].
24. O. Philipsen and A. Sciarra, *Finite size and cut-off effects on the Roberge-Weiss transition in $N_f = 2$ QCD with Staggered fermions*, 2019, arXiv:1909.12253 [hep-lat].
25. C. Bonati, G. Cossu, M. D'Elia, and F. Sanfilippo, *The Roberge-Weiss endpoint in $N_f = 2$ QCD*, Phys. Rev. D **83**, 054505, 2011, arXiv:1011.4515 [hep-lat].
26. O. Philipsen and C. Pinke, *The $N_f = 2$ QCD chiral phase transition with Wilson fermions at zero and imaginary chemical potential*, Phys. Rev. D **93**, 114507, 2016, arXiv:1602.06129 [hep-lat].